Supporting Information

Revealing the hydrogen bond network effect at electrode-electrolyte interface during hydrogen evolution reaction

Chengcheng Zhong[1], Yuxuan Xiao[1], Jinxian Feng[1], Chunfa Liu[1], Lun Li[1], Weng Fai IP[2], Shuangpeng Wang[1]*, Hui Pan[1,2]**

[1]Institute of Applied Physics and Materials Engineering, University of Macau, Macao SAR, China

[2]Department of Physics and Chemistry, Faculty of Science and Technology, University of Macau, Macao SAR, China

Corresponding Author

Email address: yuxuanxiao@um.edu.mo, spwang@um.edu.mo, huipan@um.edu.mo

Experimental section

Surface treatment of A100

The A100 sample was treated in KOH solution with different concentrations (1, 3, 6 and 8 M) by applying cyclic voltammetry at a voltage range of -1.6~0.7 V with a scanning rate of 50mV s^{-1} for 200 cycles.

Material characterizations

The X-ray diffraction (XRD) was performed on the Rigaku Smartlab X-ray diffractometer with Cu K_α radiation with a scan rate of 2 degrees min^{-1}. In-situ Raman measurements were performed on a Micro Raman System (Horiba LABHRev-UV) under the excitation sources of 532 nm. Specifically, an electrochemical workstation (CHI 660E) was connected to the in-situ Raman test setup. Starting from the overpotential of 0 mV, a voltage change gradient of 20 mV was applied, and activation was carried out at the measured voltage for 1 minute before the Raman test. In-situ Fourier transform infrared absorption spectrometer (FTIR) were performed on a Shimadzu IRXross FTIR. Specifically, an electrochemical workstation (CHI 660E) was connected to the in-situ FTIR test setup (external reflection mode). Starting from an overpotential of 0 mV, a voltage change gradient of 20 mV was applied, and activation occurred at the measured voltage for 1 minute before the Raman test. Unlike the in-situ Raman test, the in-situ FTIR test includes a background scan for each measurement. Scanning electron microscopy (SEM) and X-ray energy dispersive spectroscopy (EDS) was performed on a Zeiss Sigma instrument. The chemical composition and state of elements on the surface of the sample were analyzed by X-ray photoelectron spectroscopy (XPS, Thermo Fisher Scientific) with Al Kα X-ray (hν = 1486.7 eV). Inductively coupled plasma mass spectrometry (ICP-MS) (NexION 1000G ICP-MS) was used to determine the elemental content in the electrolyte after long-term stability test.

Electrochemical measurements:

Electrochemical measurements were conducted using a three-electrode system with treated or untreated A100 as the working electrode, a Hg/HgO (1 M KOH) as the reference electrode and a graphite rod as the counter electrode on a ModuLabXM electrochemical workstation. The electrocatalytic properties were evaluated in laboratory condition (1 M KOH, room temperature) and industrial condition (6 M KOH, 60 °C). Prior to the performance tests, the samples were pre-activated via CV with the potential range of -1.4~-1.6 V (HER) and 1.6~1.8 V (OER) at a scan rate of 300 mV s^{-1} for 500 cycles. The HER and OER performance of catalysts was measured by applying linear sweep voltammetry with a sweep rate of 5 mV cm^{-1} in 1 M KOH (room temperature) or 6 M KOH (60 °C). Electrochemical impedance spectroscopy (EIS) measurements

were conducted with a frequency range from 10^{-2} to 10^{5} Hz in 1 M KOH. Long-term stability assessment was performed in an alkaline flow cell at a current density of 400 mA cm^{-2} for 500 hours in 6 M KOH (60 °C).

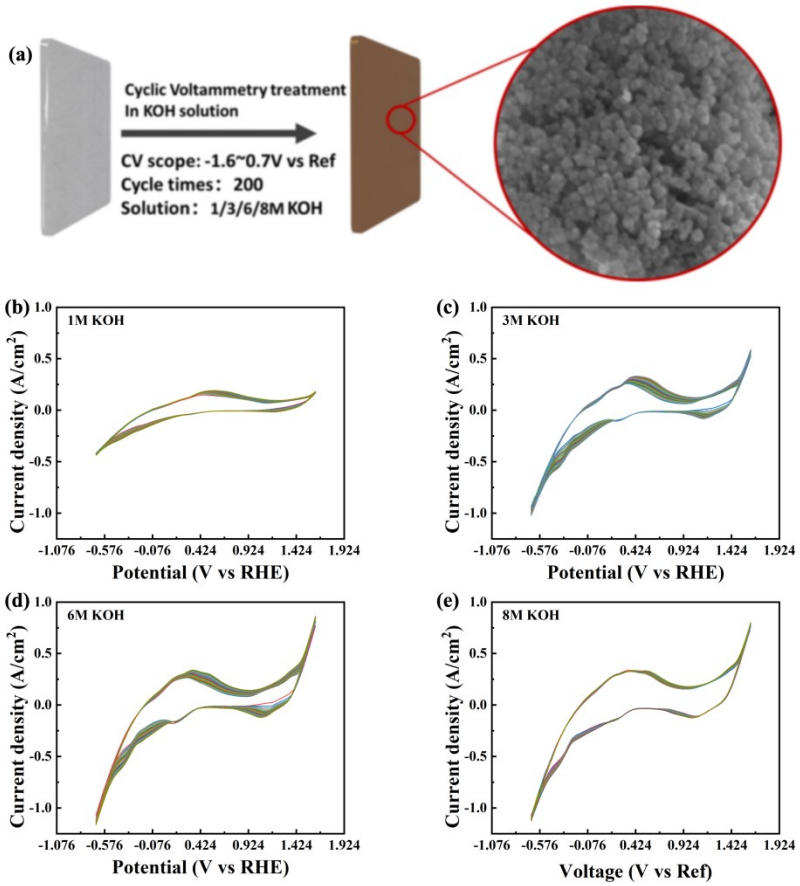

Fig. S1 (a) Schematic illustration of the treatment process of A100. CV treatment curves of (b) A100-1, (c) A100-3, (d) A100-6, and (e)A100-8, respectively.

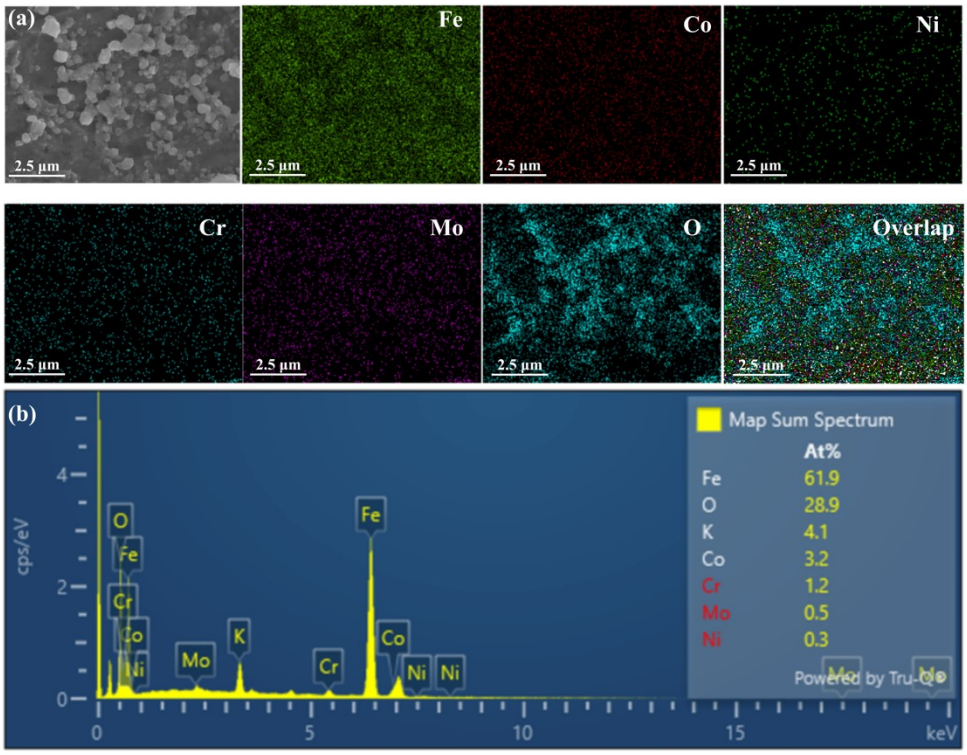

Fig.S2 (a) SEM image and EDS mapping results, and (b) EDS element atomic ratio of A100-6.

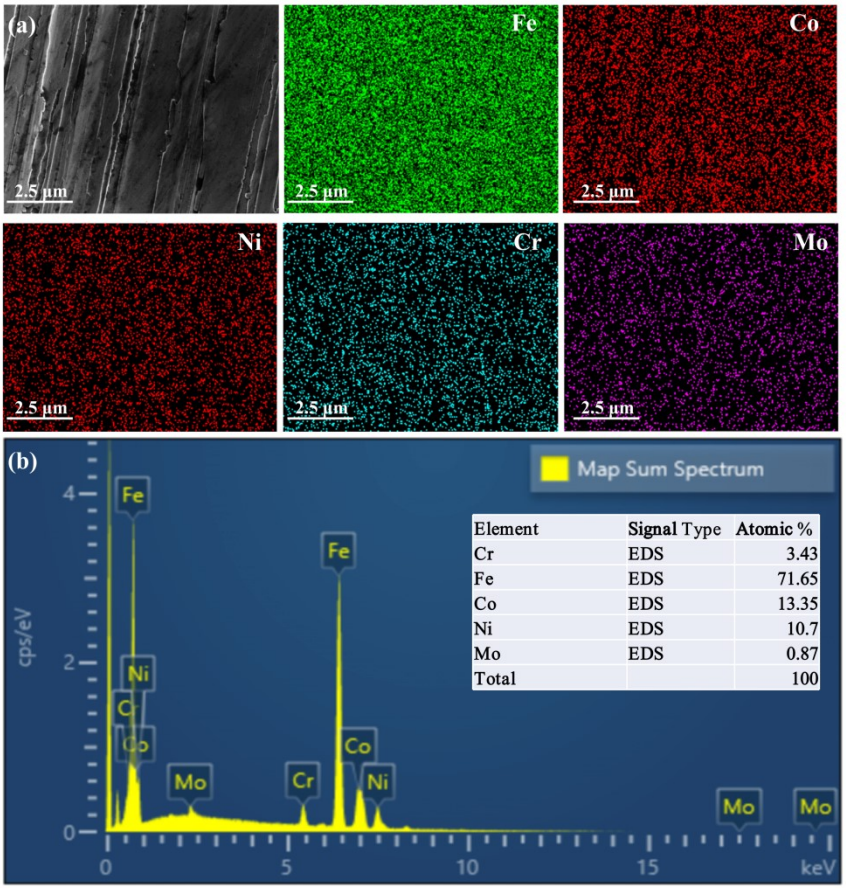

Fig. S3 (a) SEM image and EDS mapping results, and (b) EDS element atomic ratio of A100.

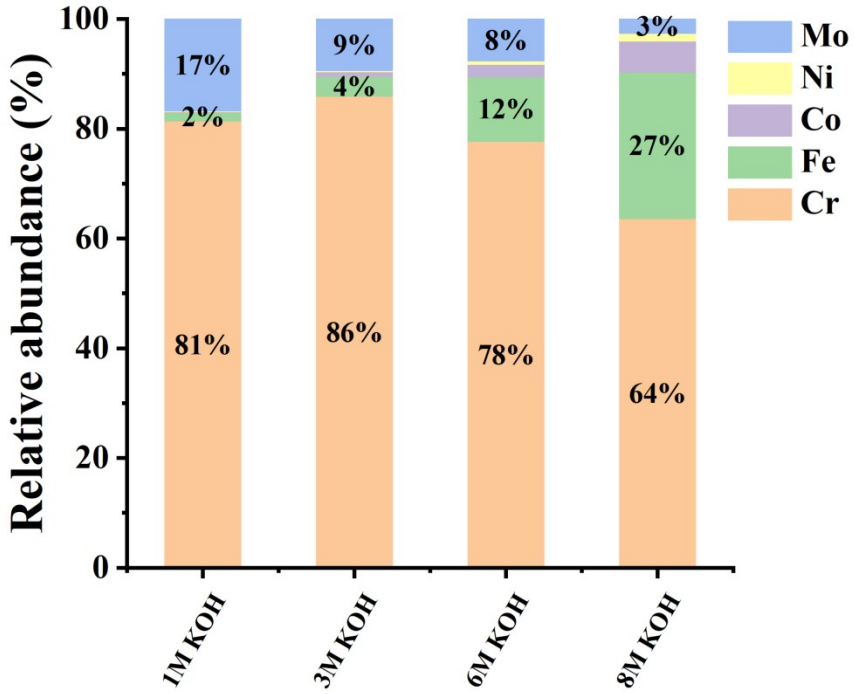

Fig. S4 ICP-MS results of dissolved metal contents in electrolyte after the CV treatment process in KOH with different concentrations.

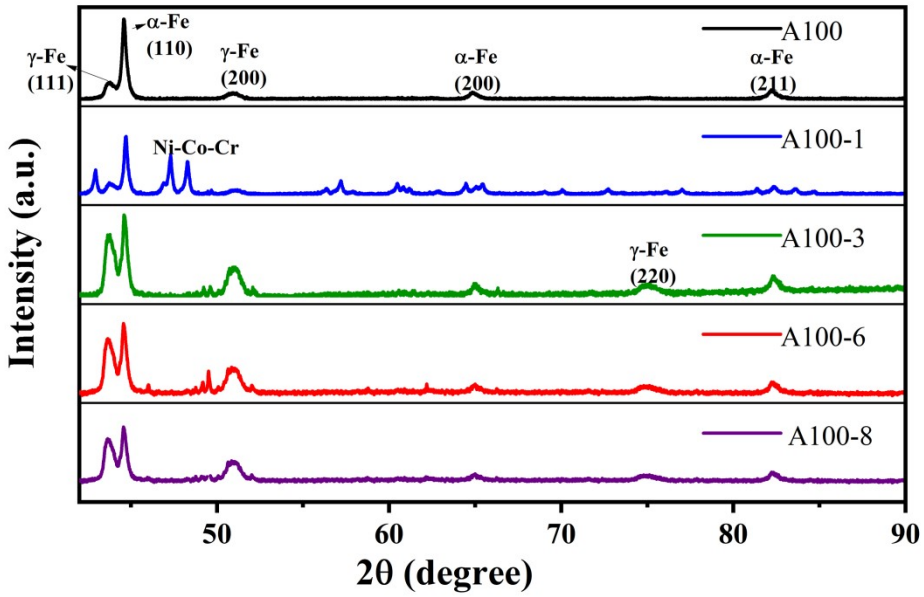

Fig. S5 XRD patterns of A100 and treated A100 samples.

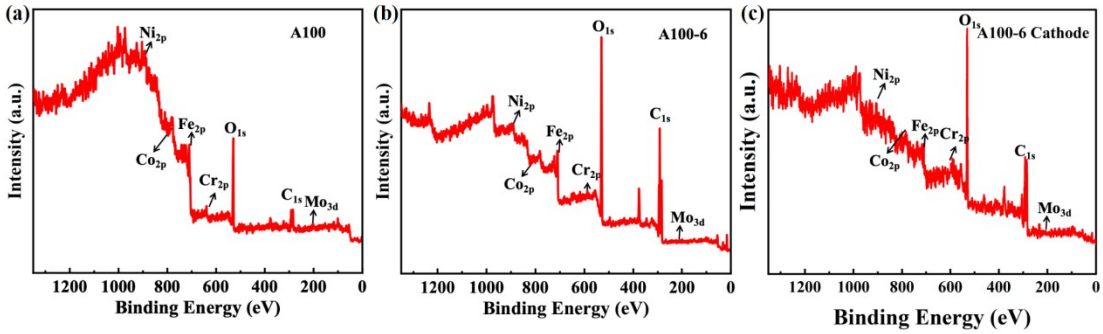

Fig. S6 The XPS survey spectra of (a) A100, (b) A100-6 and (c) A100-6 after durability test.

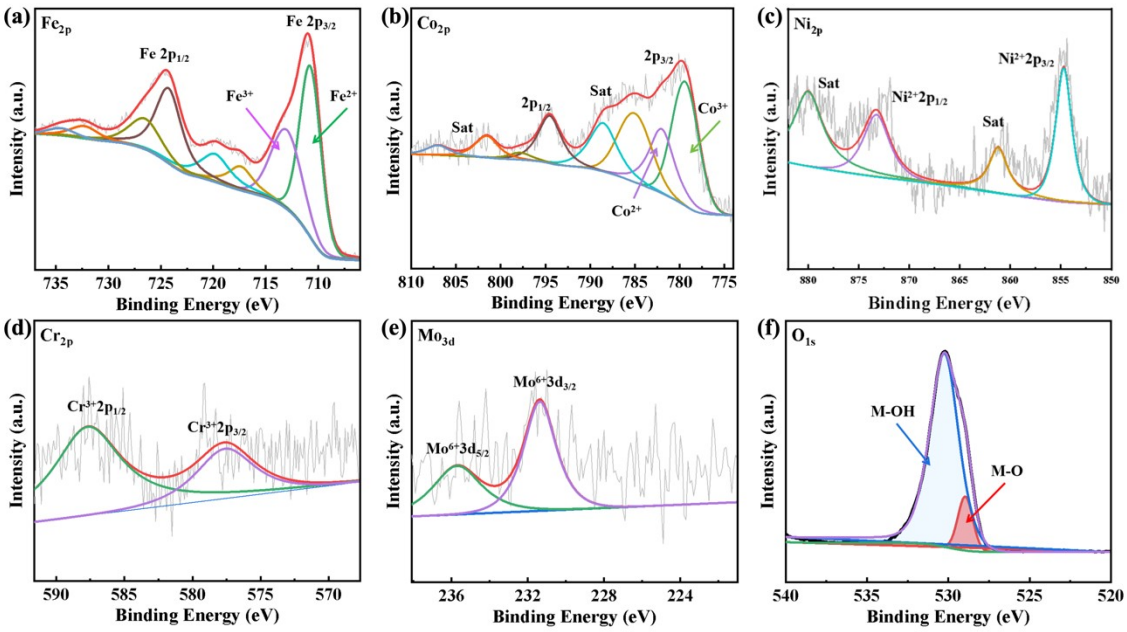

Fig. S7 The XPS data showing the (a) Fe 2p, (b) Co 2p, (c) Ni 2p, (d) Cr 2p, (e) Mo 3d, and (f) O 1s signals of A100-6.

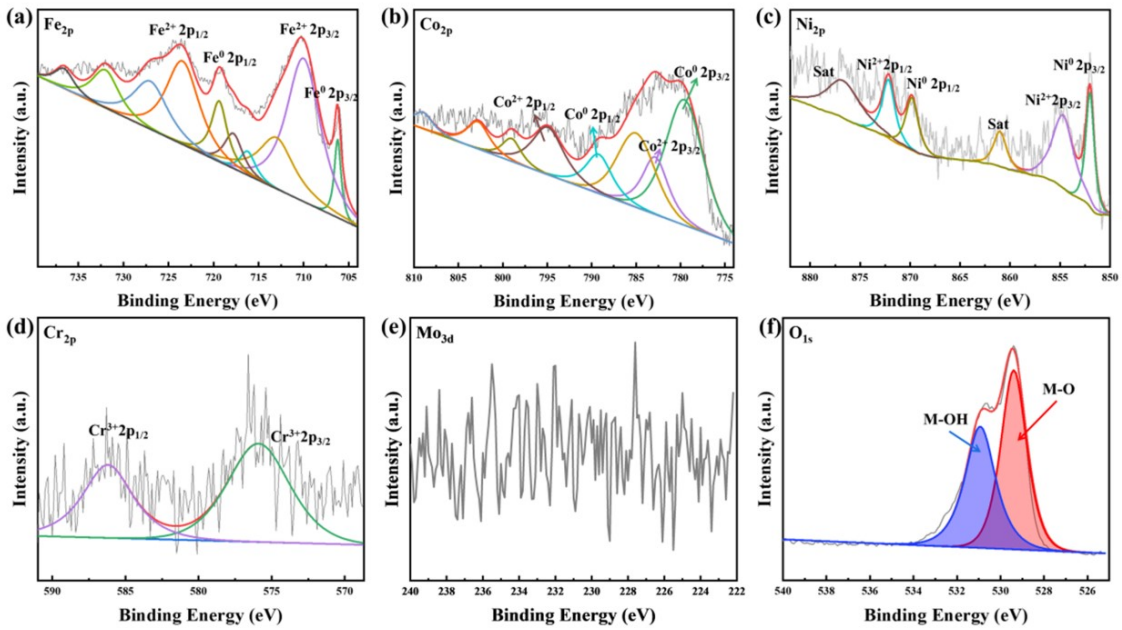

Fig. S8 The XPS data showing the (a) Fe 2p, (b) Co 2p, (c) Ni 2p, (d) Cr 2p, (e) Mo 3d, and (f) O 1s signals of A100.

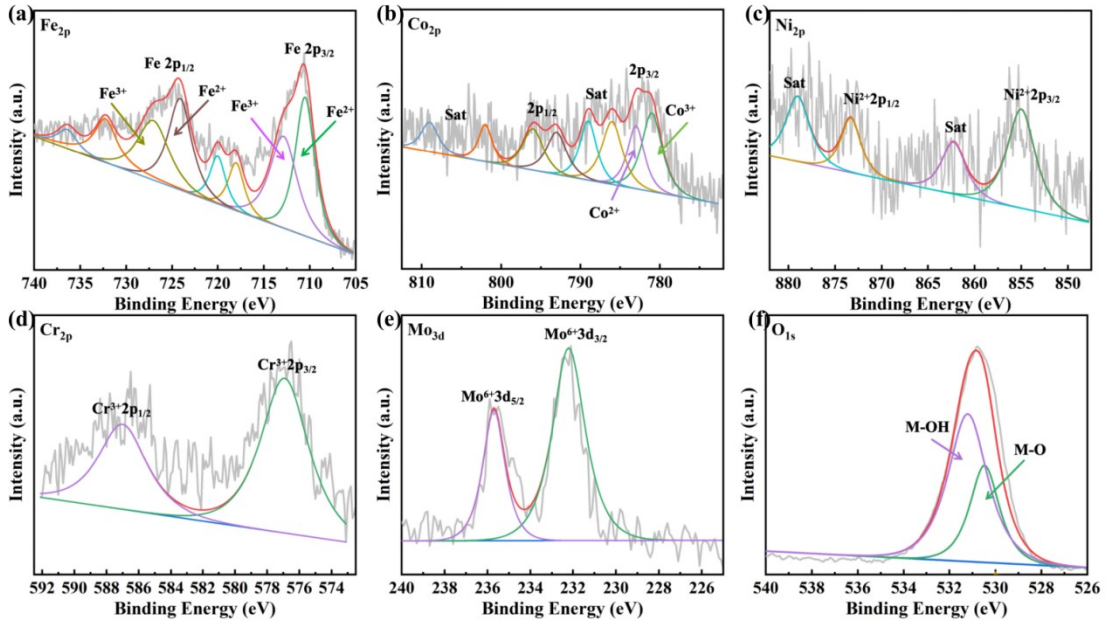

Fig. S9 The XPS data showing the (a) Fe 2p, (b) Co 2p, (c) Ni 2p, (d) Cr 2p, (e) Mo 3d, and (f) O 1s signals of A100-6 after the stability test.

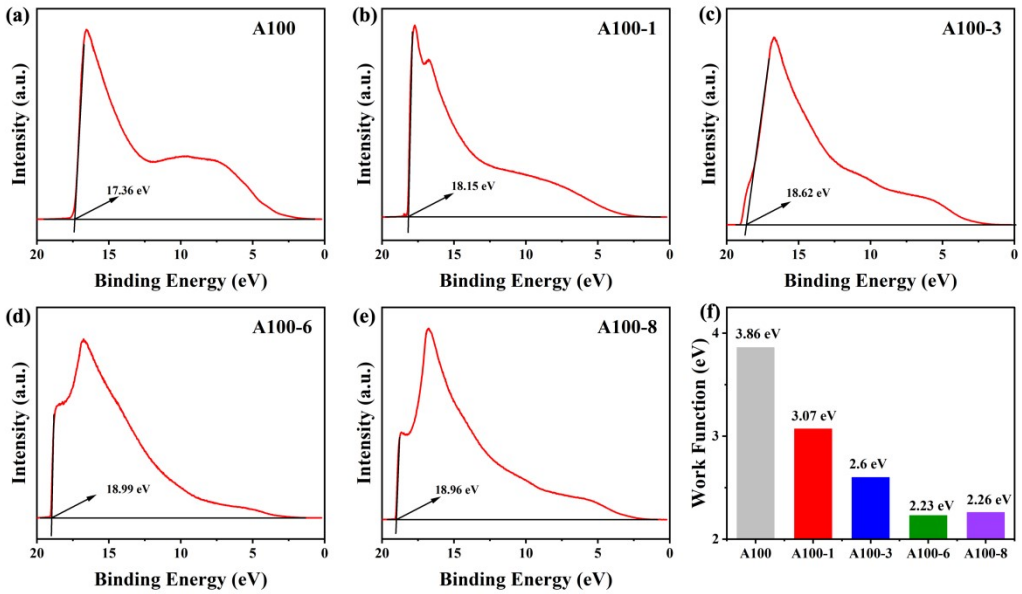

Fig.S10 UPS spectra of (a) A100, (b) A100-1, (c) A100-3, (d) A100-6 and (e) A100-8. (f) Comparison of WF values of treated and untreated A100 samples.

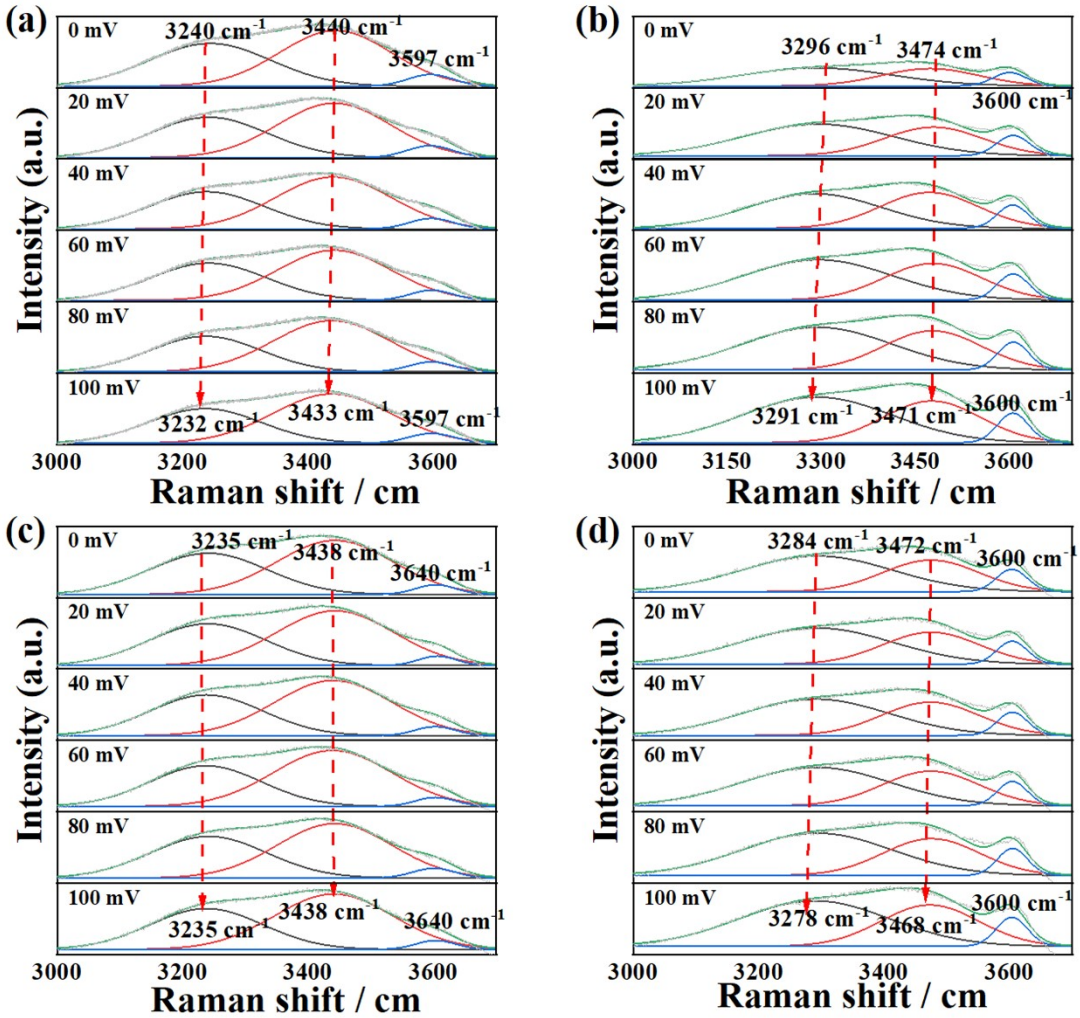

Fig. S11 Gaussian peak fitting results of the Raman peaks of water during the HER process for A100-6 in (a) 1 M KOH and (b) 6 M KOH and A100 in (c) 1 M KOH and (d) 6 M KOH.

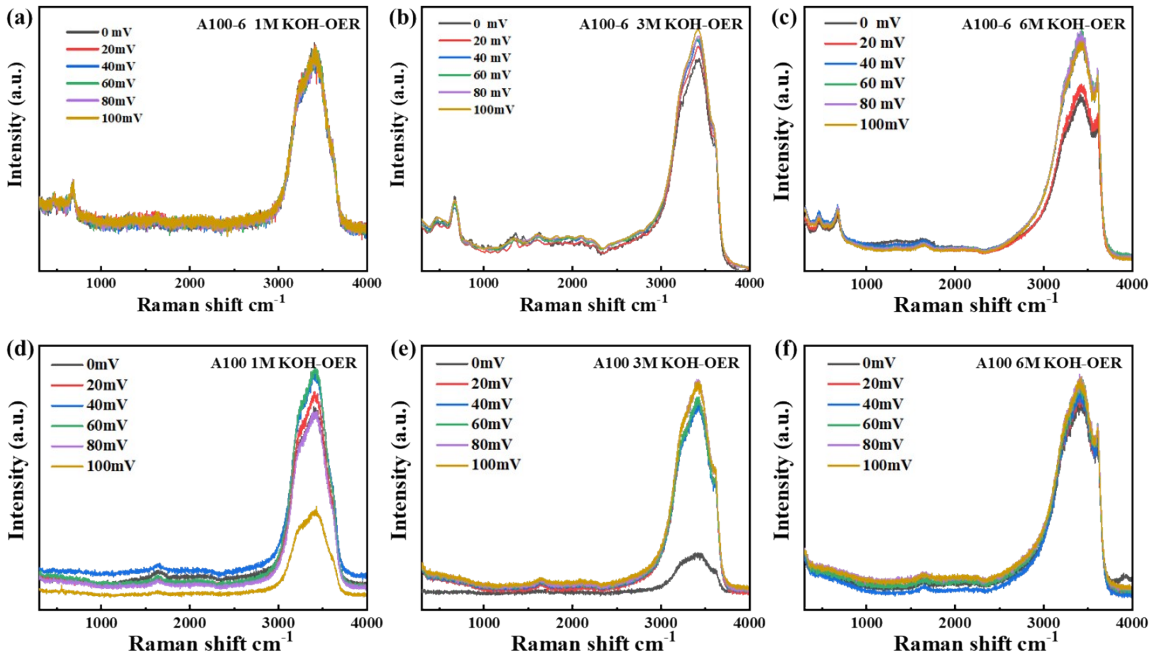

Fig.S12 In-situ Raman spectra (OER process) of A100-6 in (a) 1 M KOH, (b) 3 M KOH and (c) 6 M KOH solution. In-situ Raman spectra (OER process) of A100 in (d) 1 M KOH, (e) 3 M KOH and (f) 6 M KOH solution at different overpotentials.

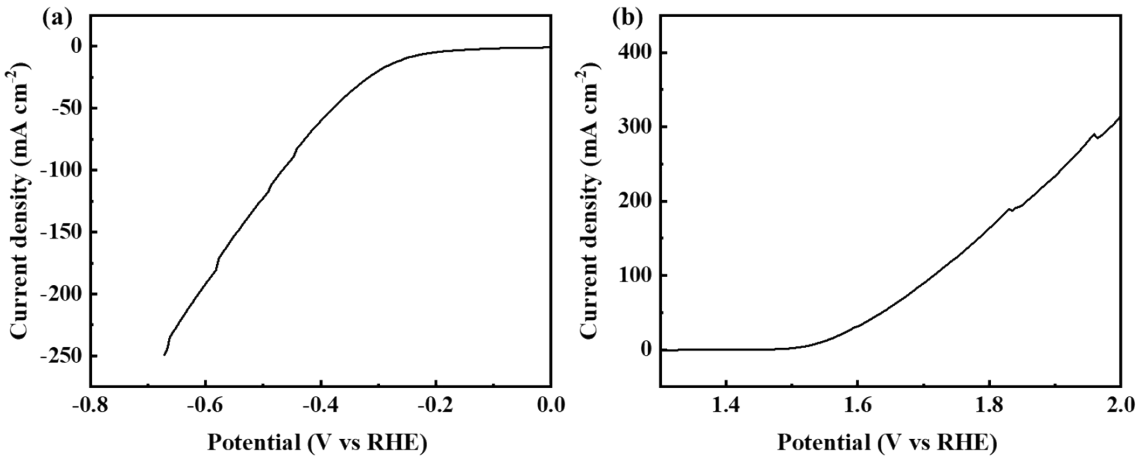

Fig.S13 (a) HER and (b) OER polarization curves of industrial nickel net in laboratory condition (1 M KOH and ambient temperature).